Available online at www.sciencedirect.com
SCIENCE DIRECT®
Proceedings of the Combustion Institute 30 (2005) 2131–2139
Proceedings of the Combustion Institute
www.elsevier.com/locate/proci

Absolute radical concentration measurements in low-pressure H_2/O_2 flames during the combustion of graphite

T. Bohm[a,*], N. Ditzian[b], G. Peiter[a], H.-R. Volpp[a], S. Cheskis[b], J. Wolfrum[a]

[a] *Physikalisch-Chemisches Institut, Universität Heidelberg, Im Neuenheimer Feld 253, D-69120 Heidelberg, Germany*
[b] *School of Chemistry, Sackler Faculty of Exact Sciences, Tel Aviv University, Ramat Aviv, Tel Aviv 69978, Israel*

Abstract

Absolute CN and CH radical concentrations were determined in situ during the combustion of a graphite substrate in premixed, laminar, low-pressure, H_2/O_2 flames for two different equivalence ratios, $\phi = 1.0$ and $\phi = 1.5$. For CN measurements, a small amount of NO (1.8%) was added. The concentration of CN was measured by cavity ring-down spectroscopy (CRDS) probing the absorption of the $P_{1,2}$ (13) in the B–X (0,0) band at 388.1 nm, and the concentration of CH was measured by linear unsaturated laser-induced fluorescence (LIF) exciting the fluorescence of the R_1 (4) in the B–X (0,0) band at 387.4 nm. Temperature measurements were done based on LIF excitation spectra of OH in the A–X (0,0) band. It was found that the graphite substrate reduces the flame temperature in the vicinity of its surface. The CN concentrations were found to be three times higher for the rich flame than for the stoichiometric flame. CH concentrations were slightly higher for the stoichiometric flame than for the rich flame. The observed CH/CN concentration ratio is substantially lower compared to NO-doped low-pressure CH_4/O_2 flames. The obtained quantitative information can serve as a first calibration point for detailed numerical simulations of the burning solid graphite, which are based on the concept of surface elementary reactions.

Keywords: Heterogeneous combustion; Diagnostic methods: spectroscopic, laser; Flames: laminar, premixed

1. Introduction

In coal combustion, nitrogen oxides, collectively termed NO_x, are formed either from the fixation of N_2 in the combustion air at high temperatures or from the oxidation of nitrogen chemically bound in coal. These nitrogen oxides can react with char, which results from coal combustion, reducing the NO concentration [1]. However, a detailed reaction mechanism of the latter process has not yet been established. Therefore, a detailed understanding of the elementary processes during the oxidation of carbon is of fundamental and applied interest to improve coal combustion and gasification processes. The

* Corresponding author. Fax: +49 0 6221 54 4255.
E-mail address: tbohm@pci.uni-heidelberg.de (T. Bohm).

1540-7489/$ - see front matter © 2004 The Combustion Institute. Published by Elsevier Inc. All rights reserved.
doi:10.1016/j.proci.2004.08.002

combustion of graphite in a well-defined environment can be considered as the simplest model system to study the chemical interaction and possible reduction of NO by carbon in char.

Earlier studies on these elementary processes show that O_2 molecules first interact with carbon atoms at defect sites forming oxide complexes [2,3], which can react later on with gas-phase species [4]. Recently, reaction pathways for the formation of such complexes and the formation of CO and CO_2 have been identified on graphite surfaces by means of density functional (DF) calculations [5].

Oxidation of highly orientated pyrolytic graphite (HOPG) produces etch pits on the basal plane that can be one or many graphite layers deep as studied by scanning tunneling microscopy (STM) [6]. These well-reproducible structures offer good possibilities for detailed mathematical modeling of the coupling of heterogeneous and homogeneous processes during carbon reactions. One problem of great practical interest is the reduction of the NO_x emission during the combustion of coal, which can be affected not only by the kinetics of the surface but also by the interaction between the solid and the gas phase.

Laser spectroscopy methods prove to be very important tools for the non-intrusive study of gas-phase chemistry in flames [7–9]. Their high spatial resolution allows for investigations of the boundary layer close to surfaces [10]. In addition, non-linear laser spectroscopic techniques can be applied for in situ studies of heterogeneous combustion processes at catalytic surfaces [11,12]. In the present work, absolute CN and CH gas-phase radical concentrations along the centerline of a burner were determined in situ during the combustion of graphite in premixed, laminar, low-pressure H_2/O_2 flames for two different equivalence ratios. For CN detection studies, NO was added. CN concentrations were quantified by cavity ring-down spectroscopy (CRDS) probing the absorption of the $P_{1,2}$ (13) lines around 388.1 nm, and the concentration of CH was quantified by linear unsaturated laser-induced fluorescence (LIF) exciting the fluorescence of the R_1 (4) line around 387.4 nm. In the latter case, an absolute calibration of the relative profiles was obtained by using Raman scattering to measure the optical collection efficiency while lifetime measurements corrected for quenching effects.

To the best of our knowledge, it is for the first time that absolute concentrations of CN and CH radicals have been determined in H_2/O_2 flames during the combustion of graphite. The distribution profiles of these key radicals reported in the present contribution provide quantitative data for the validation of future kinetic models, which simulate the graphite burning as well as the formation and destruction of the nitrogen oxides in such system.

2. Experimental setups and methods

2.1. Concentration measurements

Two experimental setups were employed to measure radical concentrations: the LIF measurements were performed in Heidelberg and the CRDS measurements in Tel Aviv. Both setups include the same modified McKenna burner, where the effective surface of the sintered bronze is reduced from the standard 6 to 2 cm diameter (see Fig. 1). A 5 cm diameter mount (7 mm thickness, stainless steel) with a scale was arranged above the burner to position the graphite substrate ($32 \times 32 \times 2$ mm, type R 8340, SGL Carbon) at a distance of 15, 20 or 25 mm above the burner. These distances were determined separately by measuring the positions of the graphite substrate and the burner relative to the laser beam with an accuracy higher than 0.5 mm.

Laminar, premixed H_2/O_2 flames with equivalence ratios of $\phi = 1.0$ and $\phi = 1.5$ were investigated. All experiments were conducted at a total chamber pressure of 4 kPa (30 Torr). For CN radical measurements, the flames were doped with 1.8% NO. This amount of NO was used due to the sensitivity limitations in detecting the CN radical, which is found in relatively low concentrations even in NO-seeded CH_4/O_2 flames [13]. In the Tel Aviv setup (see Fig. 2A), the burner was located in a 40 cm diameter vacuum chamber with automatic pressure regulation due to a feedback valve controller (Model 252/253, MKS Instruments) with an exhaust throttle valve. The

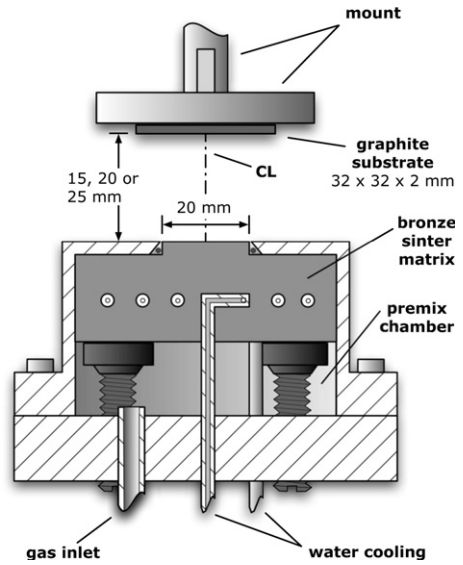

Fig. 1. Relevant dimensions of the modified McKenna burner, the graphite substrate, and its mount. CL denotes the centerline of the burner.

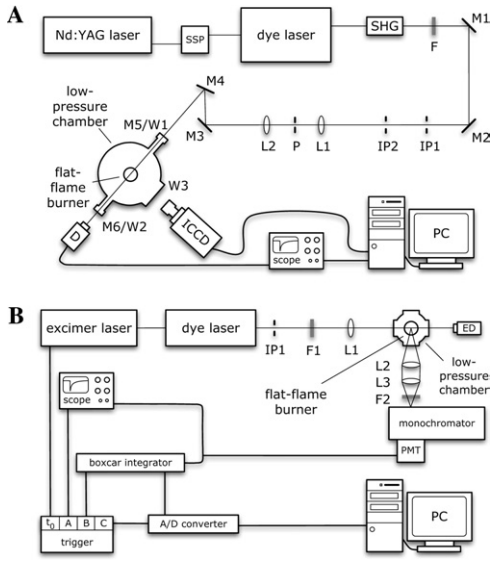

Fig. 2. Schemes of the experimental setups for the measurements (A) of the CN concentration by CRDS and the temperature determination by OH LIF measurements and (B) of the CH concentration by LIF. F, filter; M, mirror; IP, iris-pinhole; L, lens; P, pinhole; W, window; and D, detector (for CRDS: a PMT; for LIF: a photodiode), and ED, energy detector.

horizontal and vertical axes of the burner were adjustable relative to the fixed optical axis with the aid of two microstep controllers (PCI-SM32, Owis) with an accuracy of 1/64 mm. In the experiments, the burner and the mount of the graphite substrate were moved in this chamber only in the vertical axis. In the Heidelberg setup (Fig. 2B), the same burner was fixed on the bottom of a 15 cm diameter vacuum chamber. This chamber had four Suprasil windows (Ø = 7 cm) and was mounted on two independently supported *x*–*y*-tables.

Gasflows (H_2, O_2, and NO) were regulated by calibrated mass flow controllers (MKS Instruments and Millipore). The total flow of the gases was 3050 sccm and the exit gas velocity was 4 m/s. Two dry ice/acetone traps, kept at a temperature of 213 K, and a tubular oven (MRC Instruments) were used to remove traces of NO_2 from the NO added.

2.1.1. Cavity ring-down spectroscopy

CRDS is a highly sensitive absorption method based on the measurement of the light intensity decay rate in a high-quality optical cavity after injecting a light pulse from a narrowband laser into it [14,15]. CRDS may be considered as a multipass absorption technique, with an equivalent absorption path length given by the number of round trips inside the cavity before the injected intensity decays by a factor of *e*. The absorption signal k in CRDS is given by the inverse decay time

$$k = 1/\tau = (T + \Lambda + \sigma(\lambda)nl)c/L, \quad (1)$$

where $T + \Lambda$ are the cavity losses due to the transmission (T), absorption and scattering (Λ) of the mirrors, $\sigma(\lambda)$ is the absorption cross-section at the wavelength λ of the sample placed inside the cavity at the concentration n and the effective length l, c is the velocity of light, and L is the length of the cavity. The effective length l close to the graphite surface was determined experimentally by radial CH-profiles obtained by LIF. In laminar flames, CH radicals are suitable for locating the flame front [16] and, therefore, also appropriate for characterizing the reaction zone of the graphite combustion. It was found that in the boundary layer in which the CN radicals can be detected l corresponds with the dimensions of the graphite substrate.

For good spatial resolution, it was necessary to match the mode of the excitation laser beam with the cavity mode so that the light injected into the cavity mostly belongs to the lowest order TEM_{00} mode. This was done using two lenses L1 and L2 (f = 100 mm) and a 50 μm pinhole P (Fig. 2A).

The optical port of the CRDS apparatus contained two long arms connected to the low-pressure chamber by stainless steel edge-welded bellows. These arms were closed by two concave high-reflectivity mirrors M5 and M6 (R > 99.94%, radii of curvature: 0.5 m, Layertec) forming a ring-down cavity of 84 cm in length. A weak flow of nitrogen (100 sccm) was added through thin tubes near the mirrors to reduce contamination of the mirrors by combustion products.

The third harmonic of a pulsed Nd:YAG laser (Surelite I-10, Continuum) with a repetition rate of 10 Hz pumped a dye laser (ND-60, Continuum) that was operated in the range of 388–390 nm with the LD390 dye (Exciton).

The ring-down signal was observed through mirror M6 by a photomultiplier tube (R 2693, Hamamatsu) and a UV filter (U-340). The signal was fed to a LeCroy oscilloscope and transferred to a personal computer (PC) for processing after averaging 100 consecutive laser pulses.

2.1.2. Laser-induced fluorescence

To excite the CH B–X (0, 0) band near 388 nm, XeCl-excimer laser (LPX 200, Lambda Physik) pumped a vertically polarized FL 3002 dye laser (Lambda Physik) operating with the BBQ dye.

After passing the aperture IP1 and a variable gray filter F1 (LOT Oriel), the laser beam was focused into the chamber to a diameter of 260 mm by a collimator lens L1 (f = 350 mm), as schematically depicted in Fig. 2B. A pyroelectric energy detector ED (RjP 735, Polytec) was used to

measure the energy of the laser beam emerging from the chamber.

The emitted fluorescence was collected by two collimator lenses with foci of 150 (L2) and 350 mm (L3), respectively. After passing a long pass filter F2 (KV 418, Schott) and a monochromator (DK 480, Digikröm) to mask out the excitation laser, the LIF signal was detected by a photomultiplier tube (R 4332, Hamamatsu). This signal was processed by a boxcar integrator (SRS 250), digitized by an A/D converter (BNC 2090, National Instruments), and recorded by a PC. The system was controlled by a DG 535 trigger generator (SRS) and running at a repetition rate of 10 Hz.

The relationship between the detected signal S_{LIF} and the CH concentration N_{CH} is given by [17,18]

$$S_{LIF} = N_{CH} f_B B \Gamma \tau_{eff} E_L \alpha / (4\pi c \Delta \nu_L \tau_0), \quad (2)$$

where f_B is the Boltzmann factor, B is the Einstein absorption coefficient for the excited rovibronic transition, Γ is the line shape overlap, E_L is the laser energy, α is a function of the optical collection and transmission efficiency, c is the velocity of light, and $\Delta\nu_L$ is the laser bandwidth. τ_0 represents the natural fluorescence lifetime of the probed transition. To obtain absolute concentrations from the LIF signal, the effective lifetime τ_{eff} had to be determined. This was done by direct measurement of the total fluorescence decay time of the excited transitions as a function of the position in the flame to account for the specific collisional quenching environment. The remaining unknown factor α was determined from the slope of the Raman scattering signal intensity S_{Raman} as a function of the product of the number density N_{N_2} of nitrogen and the laser energy E_L [17,18]

$$S_{Raman} = (\partial\sigma/\partial\Omega)(N_{N_2} E_L \alpha / (hc\nu_{Raman})). \quad (3)$$

In the Raman calibration measurements, excitation and detection geometry, filter selection, and electronic settings of the PMT/gated integrator are kept the same as in the LIF measurements. To make sure that the entire LIF signal as well as the entire Raman calibration signal is detected, the gate of the boxcar integrator was set to 400 ns. For the absolute calibration measurements, the R_1 (4) transition of CH at 387.4 nm was selected.

2.1.3. Temperature measurements

The rotational temperature of OH radicals was measured with a frequency-doubled output of a dye laser operating with DCM at 614 nm and pumped by the second harmonic of the Nd:YAG laser. The beam was injected into the chamber through mirror M4 (see Fig. 2A). The energy range of the laser injected was 150–200 nJ coinciding with the linear LIF regime. The LIF signal of OH was collected with a UV lens ($f = 50$ mm, Hamamatsu) and detected by an intensified charged coupled device (ICCD) camera (PI-MAX, Princeton Instruments) from a quartz viewport W3 (VP-300QZ, MDC Vacuum products) perpendicular to the optical path of the LIF excitation laser beam.

3. Results and discussion

3.1. CN radical concentrations

Figure 3A shows a typical experimental CN spectrum of the P-branch obtained by CRDS in the $\phi = 1.5$ H_2/O_2 flame at a distance of 15 mm between the graphite substrate and the burner. The measured spectrum (Fig. 3A) corresponds very well to the simulated LIFBASE spectrum shown in Fig. 3B. The line marked by an asterisk was used for the concentration measurements.

The examined peak results from an overlap of the two spin components of the P-branch of the B–X (0,0) rovibronic transitions of CN for $N = 13$. Values for the Einstein coefficients of these transitions were obtained from the LIFBASE program [19]. In the CN concentration profile measurements, a small range of the CRDS spectra, which includes the P (13) lines as well as the baseline close to it, was recorded. It is important to know the baseline at each position because the absorption losses are very small and changes in the background ring-down time at different locations in the flame can vary with distance.

The absorbance signal measured by CRDS for individual rotational levels corresponds to the relative population number density of those levels. To relate the relative number density to the total number density of the absorbing molecule, it is required to know the gas temperature. Temperature profiles

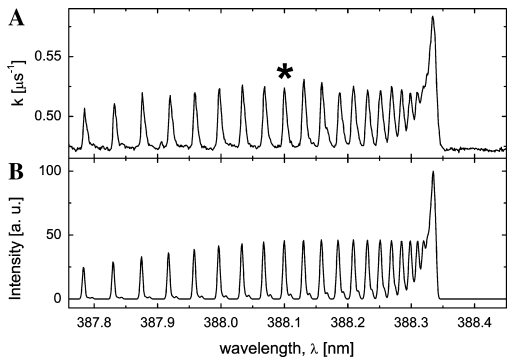

Fig. 3. (A) A cavity ring-down spectrum (resolution: 0.001 nm) near 388 nm measured at a distance of $d = 15$ mm between graphite and burner, 2 mm below the graphite surface in the 4-kPa $\phi = 1.5$ $NO/H_2/O_2$ flame in comparison with (B) the LIFBASE simulation at 1500 K. The P (13) lines excited are marked by an asterisk.

were obtained from the recorded LIF spectra of OH A–X (0, 0) band. We used a 20 ns detector gate, which is short compared to the fluorescence lifetime of OH [20]. By using such a short gate promptly after the laser pulse, the quantum yield variation with the rotational level can be neglected since very little quenching occurred. Furthermore, since the gate was switched off during the laser pulse blocking the scattered light, we did not have to use any additional spectral filtration. Thus, we avoided other problems related to the spectral limitation of the fluorescence light. The OH rotational temperature was measured employing the R-branch spectral region (306.65–307.03 nm) at each of the distances between the graphite substrate and burner for both stoichiometries (see Fig. 4). Figure 4 shows that close to the graphite surface the temperature of the flame decreases. This decrease can be due to heat losses through the graphite substrate mount, to aerodynamic changes in the vicinity of the graphite surface, as well as to changes originating from heterogeneous chemical kinetics. The temperature of the graphite substrate surface was measured with a pyrometer for different distances between graphite substrate and burner (15–40 mm) and for both stoichiometries. The highest temperature measured was about 1050 K at a distance of 15 mm between graphite and burner in the stoichiometric flame, which coincides with the gas-phase measurements. Numerical reactive flow simulations, which include heterogeneous chemistry of the graphite combustion process, are clearly necessary to obtain a theoretical description of the influence of the graphite substrate on the flame temperature. The temperature measured in the stoichiometric flame is higher than that measured in the rich flame.

We have investigated the concentration distribution of the CN radicals along the centerline (denoted as CL in Fig. 1) of the burner during the combustion of graphite in H_2/O_2 flames doped with 1.8% of NO for three different distances between the burner and the graphite substrate: 15, 20, and 25 mm.

Figure 5 shows the height profiles of the CN concentration for three different distances between graphite substrate and burner for the rich and the stoichiometric flame. In the rich flame ($\phi = 1.5$), the absolute CN concentrations were found to be about three times higher than those in the stoichiometric flame ($\phi = 1.0$), although the burning

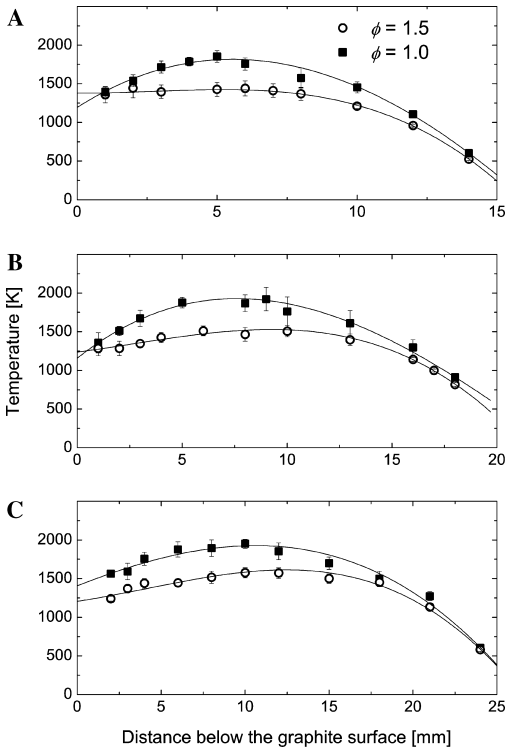

Fig. 4. Temperature profiles measured by OH LIF for a distance, d, between graphite and burner of (A) $d = 15$ mm, (B) $d = 20$ mm, and (C) $d = 25$ mm for both stoichiometries of the 4-kPa $NO/H_2/O_2$ flame. The black lines are polynomial fits of the experimental data.

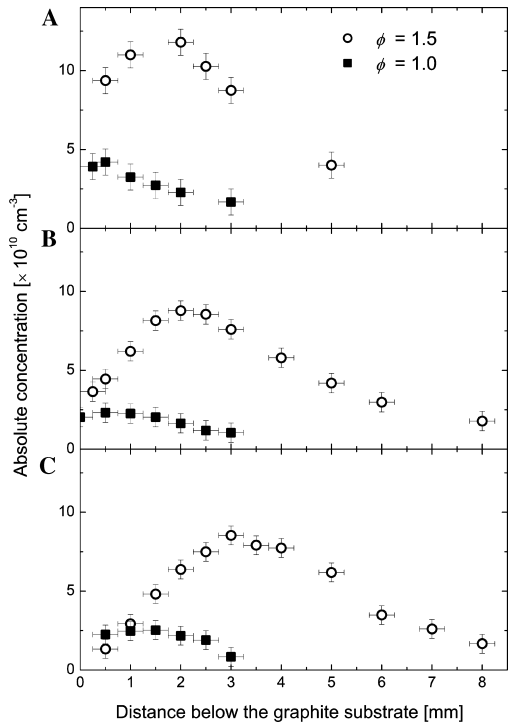

Fig. 5. Absolute CN concentrations vs. distance below the graphite substrate at the center of the 4-kPa $NO/H_2/O_2$ flames at (A) $d = 15$ mm, (B) $d = 20$ mm, and (C) $d = 25$ mm distance between the graphite substrate and the burner.

Table 1
Maximum concentrations of CN radicals in molecules/cm^3 obtained by CRDS for three different distances between the graphite substrate and the burner during the combustion of graphite in the stoichiometric ($\phi = 1.0$) as well as in the rich ($\phi = 1.5$) 4-kPa NO/H_2/O_2 flame

ϕ	15 mm	20 mm	25 mm
1.0	4.2×10^{10}	2.3×10^{10}	2.5×10^{10}
1.5	1.2×10^{11}	8.8×10^{10}	8.5×10^{10}

rate of the graphite and the temperatures were found to be significantly higher in the latter flame.

Figure 5 also indicates that the position of the maximum of the concentration profile depends on the distance between graphite substrate and burner. With decreasing distance the maximum shifts closer to the graphite surface. This change in the maximum position varies between 1 and 1.5 mm for the different distances. Table 1 summarizes the results of the maximum concentrations of CN obtained for different distances between graphite and burner at two equivalence ratios. Increasing the distance between graphite substrate and burner from 15 to 20 mm decreases the maximum concentration by a factor of about 1.5, further increasing of the distance does not substantially affect the maximum concentration anymore.

A detailed numerical study of a CH_4/air/graphite system was performed by Egolfopoulos [21] for $\phi = 0.7$, 1.0, and 1.3 flames, and for different aerodynamic strain rates. The results obtained indicate that the gas-phase equivalence ratio has a significant effect on the NO_x production and reduction and that the NO concentration is controlled by N-radical-producing reactions in the main flame zone as well as on the solid surface. Since in the latter case the carbon atoms can originate from CH_4 as well as from graphite, it is difficult to compare the results of this study with the present ones.

3.2. CH radical concentrations

CH radical concentration measurements for a distance of 25 mm between the graphite substrate and the burner were performed in the same H_2/O_2 flames as described above, however, in these studies no NO was seeded. The same spectral range that was used for CRDS observation of CN radicals also contains lines of the CH (B–X) spectral transition. The latter transition was used in several studies for CH concentration measurements employing both, CRDS and LIF [13,17,18,22–25]. In the present work, we were able to observe CH lines in a low-pressure CH_4/O_2/N_2 flame using CRDS but we could not observe any CH lines in the experiments with graphite in a NO-seeded H_2/O_2 flame. For the latter system, we estimated the maximum CH concentration to be less than 2.4×10^{11} molecules/cm^3. At this point it should be noted that the detection limit for CN radicals is at least 10 times lower than that of CH, due to the larger absorption coefficient of the former ones.

To determine absolute CH radical concentrations, LIF measurements along with a N_2 Stokes–Raman scattering calibration measurement were performed [23]. The LIF experiments were carried out under linear excitation conditions. This was verified for the R_1 (4) transition by plotting the LIF signal intensity vs. the excitation laser energy. With regard to the best signal intensity under linear conditions an excitation laser energy of 20 μJ was chosen. The presence of linear excitation conditions was validated by checking the CH LIF signal linearity in a second, independent experiment using a experimentally well-characterized CH_4/O_2 flame [24].

Absolute CH radical concentration profiles obtained for the two H_2/O_2 flames ($\phi = 1.0$ and $\phi = 1.5$) for a graphite substrate/burner distance of 25 mm are depicted in Fig. 6.

In the concentration measurements, the R_1 (4) line of the B–X (0,0) rovibronic transition of CH around 387.4 nm was excited with the fluorescence of the B–X (0,1), A–X (0,0), and (0,1) transitions at 420–440 nm being detected. In the LIF measurements, the laser was scanned over the complete spectral line to account for possible background signals.

For evaluating absolute CH concentrations from the relative concentration measurements, it was not only necessary to calibrate the LIF signal by Raman scattering but also to measure the effective fluorescence lifetime to account for fluorescence quenching effects. As shown in Fig. 7, for both H_2/O_2 flames an average value of 29 ± 5 ns was found for the effective fluorescence lifetime τ_{eff} of the (CH (B) R_1 (4)) transition at different distances below the graphite substrate.

Figure 6 shows the height profiles of the CH concentration for both flame stoichiometries for

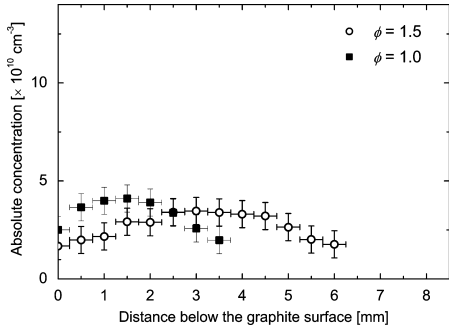

Fig. 6. Absolute CH concentrations vs. distance below the graphite substrate at the centerline of the 4-kPa H_2/O_2 flames for a distance of $d = 25$ mm between the graphite substrate and the burner.

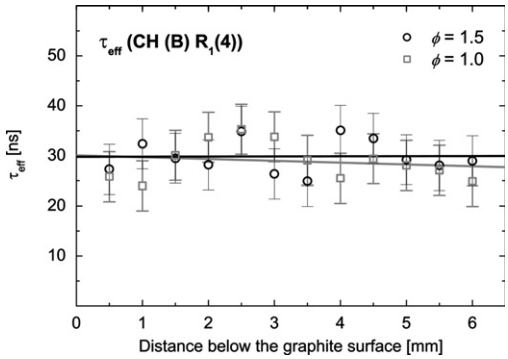

Fig. 7. Effective fluorescence lifetimes τ_{eff} of the (CH (B) R_1 (4)) transition vs. distance measured below the graphite substrate along the centerline of the 4-kPa H_2/O_2 flames for a distance of $d = 25$ mm distance between the graphite substrate and the burner.

a graphite substrate/burner distance of 25 mm. In the stoichiometric H_2/O_2 flame, the absolute CH concentration is slightly higher than at in the rich flame. Table 2 summarizes the maximum values of the absolute CH concentrations obtained in the present study. As we found already for the CN radical profiles obtained by CRDS, the CH radical profiles also show that in the rich flame the radical distributions span over a wider range than in the stoichiometric flame.

The absolute concentrations of CH measured for a 25 mm distance between graphite and burner agree with the values estimated by CRDS. The maximum CH concentration found in the stoichiometric flame ($\phi = 1.0$) is about four times lower than the minimum detectable level reached by our CRDS system. Calculations indicated that using mirrors with higher reflectivity would improve sensitivity at least by one order of magnitude. This might allow measurements of absolute CH concentrations by CRDS also in case of the NO seeded flames, which would provide further data for a better understanding of the CN formation channel(s). It is worth noting that in CH_4/O_2 flames [13] and $CH_4/O_2/N_2$ flames [26,27] seeded with similar amounts of NO, the CN concentration was found to be much lower than that of CH. The main route for the CN formation in the $CH_4/O_2/N_2$ flame doped by NO is the reaction CH + NO → HCN + O followed by the reactions of HCN with H and OH [13,25,28]. Thus, in graphite combustion there are most probably further heterogeneous surface reaction channels operating, which lead to the production of CN.

Table 2
Maximum concentrations of CH radicals in molecules/cm^3 obtained by LIF for a distance of 25 mm between the graphite substrate and the burner during the combustion of graphite in the stoichiometric ($\phi = 1.0$) as well as in the rich ($\phi = 1.5$) 4-kPa H_2/O_2 flame

ϕ	25 mm
1.0	4.1×10^{10}
1.5	3.5×10^{10}

4. Conclusions

During the combustion of solid graphite in low-pressure H_2/O_2 flames with two different stoichiometries ($\phi = 1.0$ and $\phi = 1.5$), absolute concentrations of carbon containing gas-phase radicals were measured in situ employing two different laser spectroscopic techniques. CN radicals were detected by CRDS after doping the flames with 1.8% NO. This method allows the direct determination of absolute concentration values. CH radicals were detected by LIF in undoped H_2/O_2 flames, and absolute CH concentrations were obtained after employing a N_2-Raman scattering calibration scheme.

The CN concentrations are in the rich flame ($\phi = 1.5$) by a factor of 3 higher than in the stoichiometric flame. This observation is surprising since the CN concentration grows dramatically in the rich flame in spite of the lower graphite burning rate and temperature. Therefore, additional experiments and comparisons with model calculations must be performed to clarify this effect. We also observed an increase in the CN concentration with decreasing distance between the graphite substrate and the burner. In contrast to that, the CH concentration in the stoichiometric flame is higher than in the rich flame but to a smaller extent.

The observed CH/CN concentration ratio is substantially lower if compared to NO-doped low-pressure $CH_4/O_2/N_2$ flames or CH_4/O_2 flames [13,26,27]. The higher concentration of CN observed during the combustion of graphite in NO-doped H_2/O_2 flames indicates that heterogeneous reactions of NO with the graphite surface might contribute substantially to the formation of CN under these conditions.

The present work demonstrates that quantitative information about graphite combustion gas-phase products can be obtained. These data can serve as a first calibration point for detailed numerical simulations of the combustion of solid graphite, which are based on the concept of surface elementary reactions.

Acknowledgments

This research was supported by the Israel Science Foundation (Grant No. 574/00) and by the James Franck, German-Israeli Binational

Program in Laser Matter Interaction, and the Deutsche Forschungsgemeinschaft (SFB 606).

References

[1] P. Glarborg, A.D. Jensen, J.E. Johnsson, *Prog. Energy Combust. Sci.* 29 (2003) 89–113, and references therein.
[2] R.G. Hennig, *J. Chem. Phys.* 40 (1964) 2877–2882.
[3] R.G. Hennig, *Science* 147 (1965) 733–734.
[4] A. Sibraa, T. Newbury, B.S. Haynes, *Combust. Flame* 120 (2000) 515–525.
[5] S.M. Lee, Y.H. Lee, Y.G. Hwang, J.R. Hahn, H. Kang, *Phys. Rev. Lett.* 82 (1) (1999) 217–220.
[6] L.A. Kolodny, Th.P. Beebe Jr., F. Stevens, *J. Phys. Chem.* 102 (1998) 10799–10804.
[7] K. Kohse-Höinghaus, *Prog. Energy Combust. Sci.* 20 (1994) 203–279.
[8] K. Kohse-Höinghaus, *Isr. J. Chem.* 39 (1999) 25–39.
[9] A.C. Eckbreth, *Laser Diagnostics for Combustion Temperature and Species*. Gordon and Breach, 1996.
[10] M.J. Dyer, L.D. Pfefferle, D.R. Crosley, *Appl. Opt.* 29 (1990) 111–118.
[11] T. Pery, M.G. Schweitzer, H.-R. Volpp, J. Wolfrum, L. Ciossu, O. Deutschmann, J. Warnatz, *Proc. Combust. Inst.* 27 (2002) 973–980.
[12] J. Wolfrum, *Proc. Combust. Inst.* 27 (1998) 1–41.
[13] X. Mercier, L. Pillier, A. El Bakali, M. Carlier, J.-F. Pauwels, P. Desgroux, *Faraday Discuss.* 119 (2001) 305–319.
[14] A. O'Keefe, D.A.G. Deacon, *Rev. Sci. Instrum.* 59 (12) (1988) 2544–2551.
[15] J.J. Scherer, J.B. Paul, A. O'Keefe, R.J. Saykally, *Chem. Rev.* 97 (1997) 25–51.
[16] M.G. Allen, R.K. Hanson, *Proc. Combust. Inst.* 21 (1986) 1755–1762.
[17] J. Luque, D.R. Crosley, *Appl. Phys. B* 63 (1996) 91–98.
[18] J. Luque, W. Juchmann, J.B. Jeffries, *Appl. Opt.* 36 (1997) 3261–3270.
[19] J. Luque, D.R. Crosley, *LIFBASE: Database and Spectral Simulation Program (Ver. 1.7)*, SRI International Report MP 96–001, 1996.
[20] K.J. Rensberger, J.B. Jeffries, R.A. Copeland, K. Kohse-Höinghaus, M.L. Wise, D.R. Crosley, *Appl. Opt.* 28 (17) (1989) 3556–3566.
[21] F.N. Egolfopoulos, *Int. J. Energy Res.* 24 (2000) 1257–1276.
[22] W. Juchmann, H. Latzel, D.I. Shin, G. Peiter, T. Dreier, H.-R. Volpp, J. Wolfrum, R.P. Lindstedt, K.M. Leung, *Proc. Combust. Inst.* 27 (1998) 469–476.
[23] D.I. Shin, G. Peiter, T. Dreier, H.-R. Volpp, J. Wolfrum, *Proc. Combust. Inst* 28 (2000) 319–325.
[24] P.A. Berg, D.A. Hill, A.R. Noble, G.P. Smith, J.B. Jeffries, D.R. Crosley, *Combust. Flame* 121 (2000) 223–235.
[25] J. Luque, J.B. Jeffries, G.P. Smith, D.R. Crosley, J.J. Scherer, *Combust. Flame* 126 (2001) 1725–1735.
[26] I. Derzy, V.A. Lozovsky, S. Cheskis, *Chem. Phys. Lett.* 306 (1999) 319–324.
[27] I. Rahinov, N. Ditzian, V.A. Lozovsky, S. Cheskis, *Chem. Phys. Lett.* 352 (2002) 169–175.
[28] W.C. Gardiner (Ed.), *Gas-Phase Combustion Chemistry*. Springer-Verlag, New York, 2000, p. 225.

Comments

Keith Schofield, University of California-Santa Barbara, USA. Generally, I have found that burning stoichiometric flames is not to be recommended. Practically, it is not easily achieved as flow accuracies are never exact and variations do occur. Data are likely to be more stable and reliable if slightly rich or lean conditions are chosen. This could be relevant to your CH measurements as its formation is mainly seen under fuel rich conditions and you are locating at a potentially highly variable condition.

Reply. The absolute maximum CH concentrations were found to be slightly higher in the stoichiometric flame rather than in the rich flame. Since the difference between the maximum concentrations of the two height profiles is only marginal, we do not think that small fluctuations of the gas flows are relevant to our CH concentration measurements.

•

Steve Buckley, UC-San Diego, USA. Cavity ringdown spectroscopy is extremely sensitive to particulate matter in the cavity. Do you see any evidence of aerosol formation, particularly near the graphite surface, and if so, could you quantify the aerosol mixture fraction?

Reply. No, we did not observe any evidence of aerosol formation.

•

Brian Haynes, University of Sydney, Australia. Could you please provide details on the nature and elemental composition of your graphite sample? Could some of your CN have come from nitrogen impurities in the sample? Is there any evidence of N accumulation in/on the graphite as a result of the exposure to NO?

Reply. The graphite used is an isostatically pressed specialty graphite grade R 8340 (SGL Carbon), which is for general purpose and for use as electrode material in electrical discharge machining (EDM). The average values of its physical properties are given in the table below.

The manufacturer is not providing any information about the elemental composition or nitrogen impurities so that we cannot exclude completely that some of the detected CN may originate also from nitrogen chemically bound in our graphite substrate. However, we could not detect CN in the absence of NO and therefore the amount of CN generated this way must be below the detection limit of our CRDS set-up.

We did not investigate a possible N accumulation in/on the graphite but since NO is a "sticky" molecule; we regard an N accumulation as likely.

Physical properties (average values) of the used graphite substrate (grade R 8340, SGL Carbon)

Density	1.72 g/cm^3
Porosity	15%
Average grain size	15 μm
Pore size	2.0 μm
Permeability	15×10^{-2} cm^2/s
Rockwell hardness	80 HR 10/100
Flexural strength	45 N/mm^2
Youngs modulus	10.5 kN/mm^2
Electrical resistivity	12 μΩ m
Thermal conductivity	90 W m^{-1} K^{-1}
Thermal expansion (20–200 °C)	2.9×10^{-6} (K)
Ash value	max. 0.2%